JOURNAL OF Applied Polymer SCIENCE

# Preparation and kinetic analysis of room-temperature vulcanized methylethylsilicone rubbers

**Bo Li, Zhida Zhang, Depeng Ma, Qianqian Zhai, Shengyu Feng, Jie Zhang**
Key Laboratory of Special Functional Aggregated Materials, Ministry of Education,
School of Chemistry and Chemical Engineering, Shandong University, Ji'nan 250100, People's Republic of China
Correspondence to: J. Zhang (E-mail: jiezhang@sdu.edu.cn)

**ABSTRACT:** Random copolymer poly(dimethylsiloxane-*co*-diethylsiloxane) is synthesized through anionic ring-opening polymerization. Two-component room-temperature vulcanization (RTV-2) silicone rubbers with excellent low-temperature resistance are prepared using the poly(dimethylsiloxane-*co*-diethylsiloxane) and hydrosilicone. The mechanical properties of RTV-2 rubbers with different formulas are investigated, and the optimized formula is obtained. Moreover, the curing kinetic analysis of RTV-2 silicone rubber with optimized formula is conducted using *in situ* Fourier transform infrared spectroscopy. The obtained kinetic equations are used to forecast the tack-free time at different temperatures. The results converge with the actually measured tack-free time. © 2015 Wiley Periodicals, Inc. J. Appl. Polym. Sci. **2015**, *132*, 42656.

**KEYWORDS:** applications; kinetics; rubber

Received 3 April 2015; accepted 24 June 2015
**DOI: 10.1002/app.42656**

## INTRODUCTION

Silicone rubbers have been widely used in recent years because of their excellent chemical properties, such as resistance to ozone and weathering, electrical insulating property, and excellent low-temperature resistance.[1–5] For example, high-molecular-weight poly(diethylsiloxane) (PDES) possesses a low glass transition temperature ($T_g$) of −137°C, which is the lowest for any known polymer.[6,7] However, a rigid crystal forms at temperatures below −73°C, and a conformational disorder in crystals at high temperatures limits the utilization of PDES.[8–10] Poly(dimethylsiloxane) (PDMS) also has a low $T_g$ (−123°C); however, it also has a tendency to crystallize at −40°C. Various structural modifications have been studied to obviate the crystallization of PDES or PDMS. Copolymers of dimethylsiloxane and 3,3,3-trifluoropropylmethylsiloxane are used as materials for processes at low temperatures.[7,11] The fluorinated group as a copolymerization-modified chain undermines the crystallization of the dimethylsiloxane segment. Consequently, crystallization-free copolymers with $T_g$ as low as −115°C are obtained.[7,12] Low- and high-molecular-weight poly(dimethylsiloxane-*co*-diphenylsiloxanes) have also been reported,[13] in which the $T_g$ is expected to significantly increase because the intermolecular force of the phenyl group is larger than those of the ethyl and methyl groups.[13] Similarly, poly(diethylsiloxane-*co*-diphenylsiloxane) and poly(diethylsiloxane-*co*-3,3,3-trifluoropropylmethylsiloxane),[7] as well as poly(diethylsiloxane-*co*-ethylphenylsiloxane) and poly(diethylsiloxane-*co*-methylphenylsiloxane),[8] have been reported. In addition to the aforementioned copolymers that bear two units, copolymers with three and four units have also been prepared.[6] As mentioned above, whether PDES or PDMS possesses low $T_g$. This means random copolymer of dimethylsiloxane and diethylsiloxane should have a low $T_g$. At the same time, random copolymerization could avoid crystallization at low temperature. Silicone rubbers using poly(dimethylsiloxane-*co*-diethylsiloxane) (PMES) as the gum should have excellent property of low-temperature resistance. However, only a few studies have been reported on PMES.

Curing is the key procedure in rubber processing. Curing kinetics has great guiding significance for the usability and mechanical property of the PMES-based low-temperature resistance silicone rubber. Commonly used methods for the kinetics study of rubber include physico-chemical methods,[14,15] vulcametry,[16–18] thermal analysis,[19–21] and spectrometry.[22–24] The thermal effect of curing is used as the basis in the thermal analysis of curing kinetics. A new model was proposed to study isothermal vulcanization through differential scanning calorimetry, which is defined by

$$\frac{d\alpha}{dt} = k\alpha^{m}(1-\alpha)^{n}, \quad (1)$$

where $\alpha$ is the relative reaction degree, which can be expressed as $\alpha = Qr/Qm$, where $Qm$ is the adjustable reduced parameter and $Qr$ is the heat generated in the isothermal reaction from the unreacted state to the current state; $m$ and $n$ are the constants that are unrelated to temperature; and $k$ is the constant

that is related to temperature.[19–21] In spectrometry, the position and intensity of absorption peaks of the groups involved in the curing reaction change as the reaction progresses. Structural changes and the curing mechanism can be deduced from the changes observed through Fourier transform infrared spectroscopy (FTIR). Hong *et al.*[22–24] investigated the intensity change in the absorption peak of an epoxy group during epoxy resin curing using FTIR and simplified the model as:

$$\frac{d\alpha}{dt} = k(1-\alpha)^n, \quad (2)$$

where $\alpha$ is the ratio of integral areas of the absorption peaks, $k$ represents the reaction rate constant, and $n$ represents the reaction order. $k$ and $n$ were calculated under different conditions. The kinetic equation could be obtained combining this model with Arrhenius equation to provide important guidance to practical application.

In this work, low-molecular-weight PMES copolymers (usually under a viscosity of 8000 mPa s) were synthesized through anionic ring-opening polymerization. Then, dehydrogenation cure two-component room-temperature vulcanization methylethylsilicone rubbers (RTV-2-MESR) were prepared using PMES and hydrosilicone. The low-temperature and mechanical properties were characterized.

Moreover, the curing kinetics was studied with *in situ* FTIR using eq. (2).

## EXPERIMENTAL

### Materials

Octamethylcyclotetrasiloxane ($D_4$) was purchased from Zhejiang Xinan Group Corporation (Hangzhou, China). Hexaethylcyclotrisiloxane ($D_3^{Et}$) was purchased from Weihai Xinyuan Chemical (China). Silica (S600) was supplied by Shenyang Yongxin Chemical (China). Hydrosilicone oil (1.4 wt %) was supplied by Jinan Ruiyuan Chemical (China). Dibutyltin dilaurate (DBTDL) was obtained from Tianjin Damao Chemical Reagent Factory (China).

### Synthesis of PMES

The PMES was prepared through anionic ring-opening polymerization. All glasswares were dried in an oven at 150°C for more than 4 h. The polymerization was performed in a thoroughly cleaned and dried 500 mL, three-necked, round-bottom flask. The $D_4$ and $D_3^{Et}$ were mixed in the flask, and the catalyst (1% tetramethylammonium silanolate) was added at 90°C. When the reaction mixtures became viscous, the end-capping reagent $H_2O$ was added. The viscosity of the reaction mixture decreased upon the addition of $H_2O$. The mixtures were kept at 90°C for 5 h while stirring; random copolymers were expected to be formed.[25] A transparent and viscous liquid was obtained upon the completion of the reaction. The residual monomers and low-molecular-weight oligomers were removed with vacuum distillation. The ring-opening reaction was performed as follows:

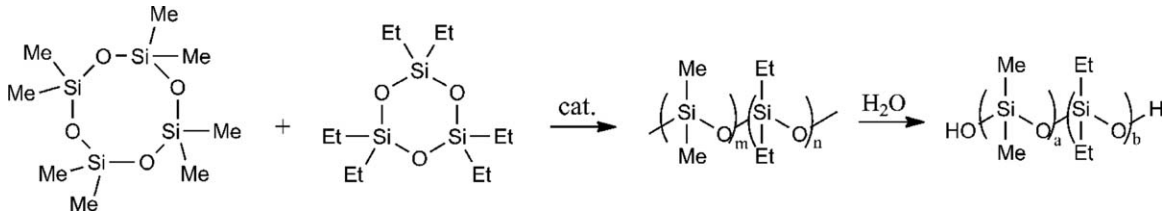


### Viscosity Test of PMES

The viscosities of PMES were tested with a NDJ-1 rotary viscometer (Shanghai Precision Instruments) at 25°C.

### FTIR Spectra Analysis of PMES

FTIR spectra were recorded on a Bruker Tensor 27 FTIR spectrometer (FTIR; Bruker) in a range of 4000–400 $cm^{-1}$. Samples were prepared as KBr pellets with 1% weight content.

### Proton Nuclear Magnetic Resonance Spectra Analysis of PMES

Proton nuclear magnetic resonance ($^1$H-NMR) spectrum was recorded on a 300 MHz Avance-300 spectrometer ($^1$H-NMR; Bruker) with $CDCl_3$ as a deuterated solvent.

### Measurement of Molecule Weight of PMES

The molecular weights of the PMES were determined by gel permeation chromatography (GPC; Water) with tetrahydrofuran as the mobile phase, the flow velocity was 1.000 mL/min.

### Preparation of RTV-2-MESR

The PMES is the gum for RTV-2-MESR. The gum and silica were mixed, and then heated at 120°C for 1 h. Upon cooling to room temperature, the mixture was divided into two parts. The hydrosilicone oil (cross-linking agent) was added to one part, and DBTDL (catalyst) was added to the other part. The two components were mixed in different proportions. Then, the mixtures were placed into the mold for curing. After a week at room temperature, RTV-2-MESR was obtained.

### Mechanical Properties

The tensile strength and elongation at break of RTV-2-MESR were measured with an XLD-A universal testing machine (Second Experimental Machine Factory) in accordance with ASTM D 412 at 25°C. The tear strength was assessed in accordance with ASTM D 624 in the same instrument.

### Differential Scanning Calorimetry Analysis

The PMES and RTV-2-MESR were evaluated with a DSC 822 differential scanning calorimetry (DSC; Mettler). The specimens were analyzed in the temperature range from −150°C to 50°C at a heating rate of 10°C/min. The Nitrogen carrier gas flow rate was 25 mL/min.

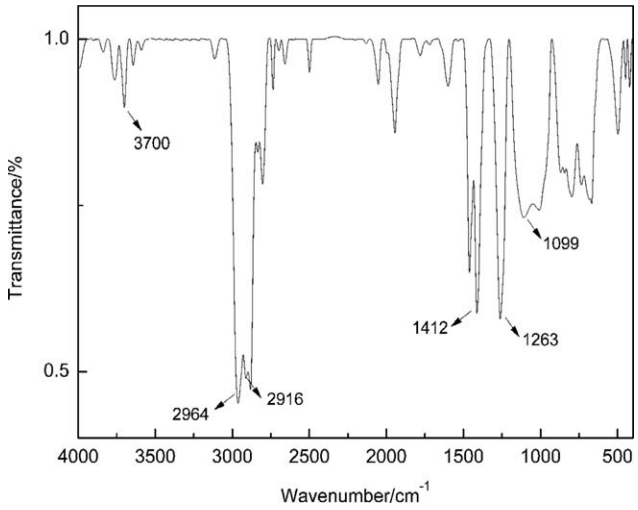


**Figure 1.** FTIR spectrum of PMES with viscosity of 6700 mPa s.

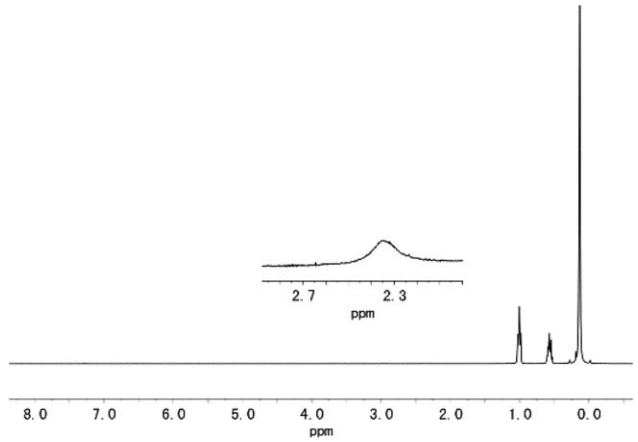


**Figure 2.** $^{1}$H-NMR spectrum of PMES with viscosity of 6700 mPa s.

### Dynamic Mechanical Analysis

The low-temperature performance of RTV-2-MESR was evaluated using an SDTA 861e dynamic mechanical analyzer (Mettler) in shearing mode. The specimens were analyzed at a frequency of 1 Hz, a temperature range of −150°C to 50°C, and a heating rate of 3°C/min.

### Measurement of Tack-Free Time

The tack-free time was measured in accordance with ASTM C 679.

### Kinetic Parameters and Kinetic Equation

The process of curing was investigated through *in situ* FTIR with a Tensor 27 FTIR Spectrometer (FTIR; Bruker) under 50% humidity. The PMES, the cross-linking agent, and the catalyst were mixed well without silica. Then, the mixtures were applied to KBr. The specimens were placed into the sample cell, and the FTIR spectra were collected every fixed time.

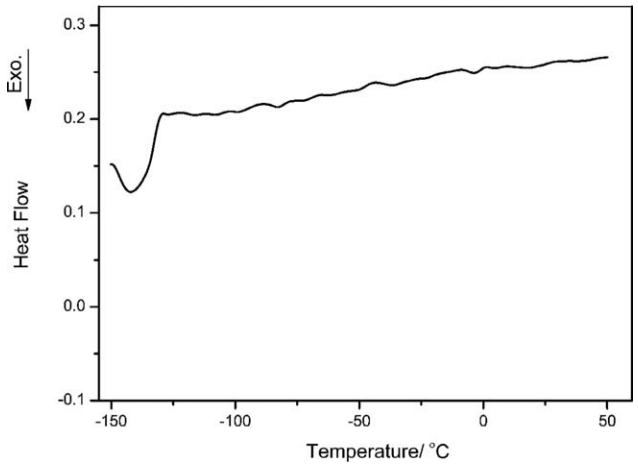


**Figure 3.** DSC curve of PMES with the viscosity of 6700 mPa s.

## RESULTS AND DISCUSSION

### Analysis of PMES

Figure 1 shows the FTIR spectrum of PMES. The peaks at 1099, 2916, 2964, and 3700 $cm^{-1}$ corresponded to the stretching vibration absorption of Si—O—Si, —$CH_2$, —$CH_3$, and —OH, respectively. The peak at 1263 $cm^{-1}$ corresponded to the deformation vibration absorption of Si—$CH_3$, and that at 1412 $cm^{-1}$ corresponded to the scissoring vibration absorption of —$CH_2$. These data indicate that the synthetic polymer is polysiloxane containing methyl, ethyl, and hydroxyl.

Figure 2 shows the $^{1}$H-NMR (300 MHz, $CDCl_3$, ppm) spectrum of PMES. The signals appearing from 0 to 0.2, 0.4 to 0.6, 0.8 to 1.0, and 2.3 to 2.4 ppm were assigned to $SiCH_3$*, $SiCH_2$*$CH_3$, $SiCH_2CH_3$*, and —OH*, respectively. These data verified the results from the FTIR spectrum. Moreover, the molar contents of methyl and ethyl can be calculated from the integral of the $^{1}$H-NMR spectrum.

PMES with different viscosities was synthesized using different amounts of end-capping reagents. Table I shows the basic information of PMES.

Figure 3 was the DSC measurement of PMES with the viscosity of 6700 mPa s. The curve had only one thermal transition (glass transition) at approximately −133°C. It indicated the PMES

**Table I.** Basic Information of PMES

| Sample | Mn (g/mol) | Mw (g/mol) | Viscosity (mPa s) | Yields (%) | Amounts of $H_2O$ (g)[a] | $Et_2OSi$ : $Me_2OSi$ |
|---|---|---|---|---|---|---|
| 1 | 11,487 | 19,641 | 2000 | 72 | 1.13 | 21 : 79 |
| 2 | 25,398 | 38,732 | 4500 | 80 | 0.57 | 20 : 80 |
| 3 | 36,552 | 54,009 | 6700 | 89 | 0.28 | 20.5 : 79.5 |

[a] With 250.12 g $D_4$, 56.03 g $D_3^{Et}$, and 5.91 g catalyst.

**Table II.** Orthogonal Design and Test Results of Mechanical Properties of RTV-2-MESR[a]

| | Factors[b] | | | | | |
|---|---|---|---|---|---|---|
| Test number | Gum viscosities | Amounts of silica | Amounts of cross-linking agent | Tensile strength (MPa) | Tear strength (kN/m) | Elongation at break (%) |
| 1 | 2000 mPa s | 10 phr[c] | 2 phr | 1.21 | 9.56 | 164 |
| 2 | 2000 mPa s | 15 phr | 4 phr | 1.62 | 10.31 | 196 |
| 3 | 2000 mPa s | 20 phr | 6 phr | 1.75 | 11.12 | 182 |
| 4 | 4500 mPa s | 10 phr | 4 phr | 2.23 | 11.93 | 212 |
| 5 | 4500 mPa s | 15 phr | 6 phr | 2.39 | 12.58 | 236 |
| 6 | 4500 mPa s | 20 phr | 2 phr | 2.46 | 13.64 | 274 |
| 7 | 6700 mPa s | 10 phr | 6 phr | 2.39 | 13.27 | 282 |
| 8 | 6700 mPa s | 15 phr | 2 phr | 2.49 | 14.87 | 312 |
| 9 | 6700 mPa s | 20 phr | 4 phr | 3.46 | 16.49 | 283 |
| Tensile strength | | | | | | |
| $K_1$ | 4.59 | 5.82 | 6.15 | | | |
| $K_2$ | 7.08 | 6.51 | 7.32 | | | |
| $K_3$ | 8.34 | 7.68 | 6.54 | | | |
| $k_1$ | 1.53 | 1.94 | 2.05 | | | |
| $k_2$ | 2.36 | 2.17 | 2.44 | | | |
| $k_3$ | 2.78 | 2.56 | 2.18 | | | |
| $R$ | 1.25 | 0.61 | 0.38 | | | |
| Tear strength | | | | | | |
| $K_1$ | 30.99 | 34.77 | 38.07 | | | |
| $K_2$ | 38.16 | 37.77 | 38.73 | | | |
| $K_3$ | 44.64 | 41.25 | 36.96 | | | |
| $k_1$ | 10.33 | 11.59 | 12.69 | | | |
| $k_2$ | 12.72 | 12.59 | 12.91 | | | |
| $k_3$ | 14.88 | 13.75 | 12.32 | | | |
| $R$ | 4.55 | 2.16 | 0.59 | | | |
| Elongation at break | | | | | | |
| $K_1$ | 542.01 | 657.99 | 750.00 | | | |
| $K_2$ | 722.01 | 744.00 | 690.99 | | | |
| $K_3$ | 876.99 | 738.99 | 699.99 | | | |
| $k_1$ | 180.67 | 219.33 | 250.00 | | | |
| $k_2$ | 240.67 | 248.00 | 230.33 | | | |
| $k_3$ | 292.33 | 246.33 | 233.33 | | | |
| $R$ | 111.67 | 28.67 | 19.67 | | | |

[a] Five samples used for each dataset in the mechanical testing, median was selected as testing value.
[b] Amounts of catalyst for all the testing samples were 1 phr.
[c] Parts per hundred rubber.

had a very low $T_g$ and no crystallization. The expected random copolymers were obtained.

### Mechanical Properties and Optimized Formula

The mechanical properties of RTV-2-MESR were studied at room temperature (25°C) by orthogonal design. Table II shows the orthogonal design and test results.

The tensile strength, tear strength, and elongation at break increased with increasing viscosities of PMES, and gum viscosity was the most important factor affecting various mechanical indices. Higher molecular weight corresponded to longer and more flexible molecular chains, and thus better mechanical properties. However, the excessive viscosity (usually higher than 8000 mPa s) of PMES resulted in poor fluidity, and made it unsuitable for RTV-2-MESR.

The tensile strength and tear strength of RTV-2-MESR increased with increasing quantities of silica. However, excessive quantity of silica led to aggregation, which resulted in the poor

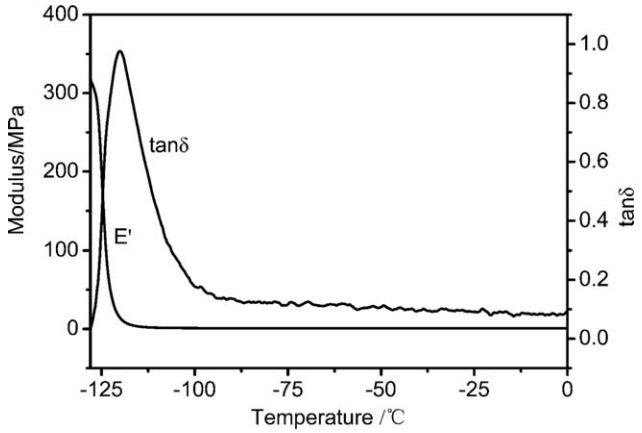


**Figure 4.** DMA measurement of RTV-2-MESR.

performance and difficult processing of RTV-2-MESR. The elongation at break decreased a little with 20 phr silica due to the increasing hardness of RTV-2-MESR.

With increasing quantities of the cross-linking agent, the tensile strength and tear strength of RTV-2-MESR initially increased and then decreased. Excessive quantity of the cross-linking agent had the effect of a chain extender instead of a cross-linking agent, which decreased the mechanical properties of RTV-2-MESR.[26] The elongation at break increased with higher or lower amounts of cross-linking agent, it could be inferred from the results that the elongation at break increased with decreasing cross-linking density.

For highest tensile strength and tear strength, the formulas were the same, that is viscosity of PMES, 6700 mPa s, 20 phr silica, 4 phr cross-linking agent, and 1 phr catalyst. The value of elongation at break was suitable with this formula, therefore this formula could be considered as the optimized formula through comprehensive comparisons using multiple compounds with varying quantities of each material.

### Low-Temperature Resistance Analysis of RTV-2-MESR

Figure 4 shows the dynamic mechanical analysis (DMA) measurements of RTV-2-MESR prepared with the above optimized formula. The DMA measurements were used to study the low-temperature performance of RTV-2-MESR.[27] The storage modulus ($E'$) and the loss factor (tan $\delta$) are shown in Figure 4. The $E'$ curve of RTV-2-MESR had only one thermal transition and sharply decreased at approximately −125°C. This result indicated that RTV-2-MESR was not crystalline. Moreover, the loss factor (tan $\delta$) curve exhibited only one peak at approximately −120°C because of the glass transition. This result demonstrated the significant low-temperature performance of RTV-2-MESR, which may be attributed to the low $T_g$ and no crystallization properties of PMES.

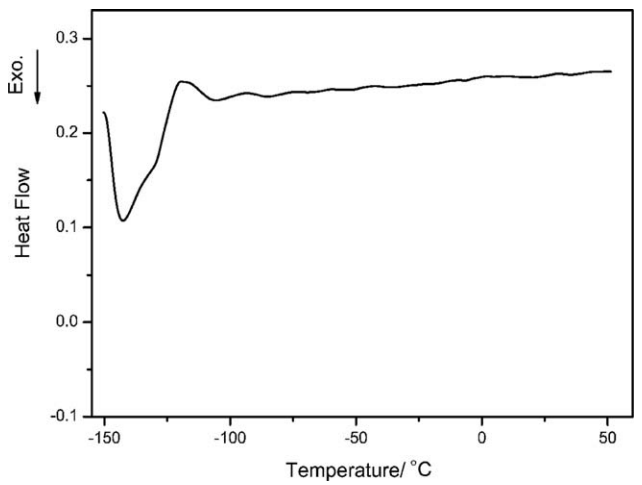


**Figure 5.** DSC measurement of RTV-2-MESR.

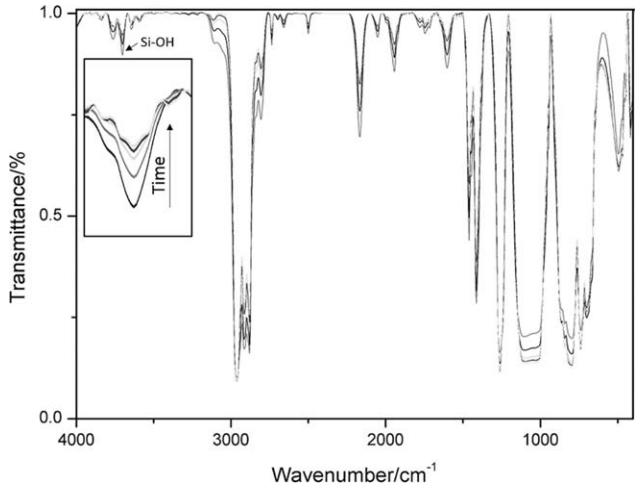


**Figure 6.** The typical FTIR spectra of RTV-2-MESR under varied curing time.

Figure 5 shows the DSC measurements of RTV-2-MESR prepared with optimized formula. The DSC curve verified the results from the DMA measurement. It exhibited only one glass transition temperature at approximately −123°C, and there is no crystallization temperature.

### Kinetics Analysis of Curing

*In situ* FTIR was used to investigate the curing of RTV-2-MESR. In the cross-linking reaction of RTV-2-MESR, polycondensation occurred between Si—OH and Si—H. The concentrations of Si—OH and Si—H decreased as the reaction progressed. Furthermore, the FTIR spectrum showed that the integral area of the absorption peaks of Si—OH and Si—H decreased as the reaction progressed. The change in the integral area of the absorption peak of Si—OH was used to investigate the polycondensation reaction. Figure 6 shows the typical FTIR spectra of RTV-2-MESR under varied curing time at 25°C with optimized formula.

Using the internal standard method, the integral area of the absorption peak of Si—$CH_3$ was used as a reference. The conversion ($\alpha$) was defined as:

$$\alpha = 1 - \frac{(A_{3700}/A_{2964})_t}{(A_{3700}/A_{2964})_0}, \quad (3)$$

where $(A_{3700}/A_{2964})_t$ is the ratio of the integral area of absorption peak at 3700 $cm^{-1}$ (Si—OH) and the integral area of the absorption peak at 2964 $cm^{-1}$ (Si—$CH_3$) at $t$ time of reaction, and $(A_{3700}/A_{2964})_0$ is the same ratio at the beginning of the reaction. The optimized formula was selected to study the curing

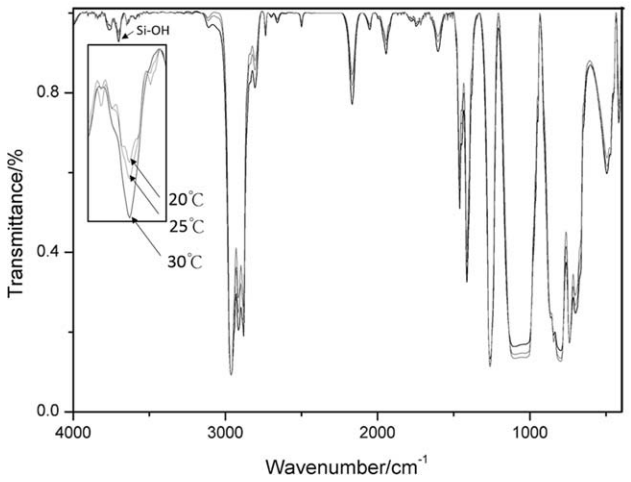


**Figure 7.** The typical FTIR spectra of RTV-2-MESR under varied curing temperature.

kinetics. Figure 7 shows the typical FTIR spectra of RTV-2-MESR under varied curing temperature at some point with optimized formula. Figure 8 shows the time versus conversion curves at different temperatures with the optimized formula.

According to eq. (2):

$$\frac{d\alpha}{dt}=k(1-\alpha)^n,$$

where $k$ represents the reaction rate constant, and $n$ represents the reaction order. Taking the natural logarithm processing of both sides of the equation, we obtain

$$\ln\left(\frac{d\alpha}{dt}\right)=\ln k+n\ln(1-\alpha). \quad (4)$$

Figure 9 shows the $\ln(1-\alpha)$ versus $\ln(d\alpha/dt)$ curves.

The values of $n$ and $\ln k$ were obtained through linear fitting. Table III shows the values of $n$ and $k$ at different temperatures.

The values of $n$ indicate the reaction obeys a second-order reaction kinetic model, and the curing rate accelerated with increasing reaction temperature. According to the Arrhenius equation,

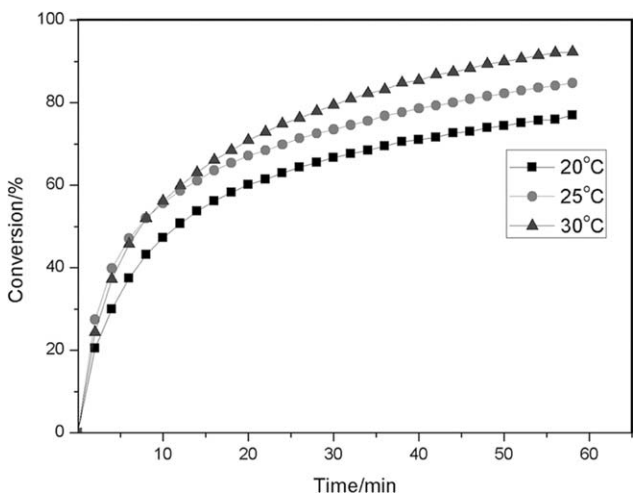


**Figure 8.** Time versus conversion curves at different temperatures.

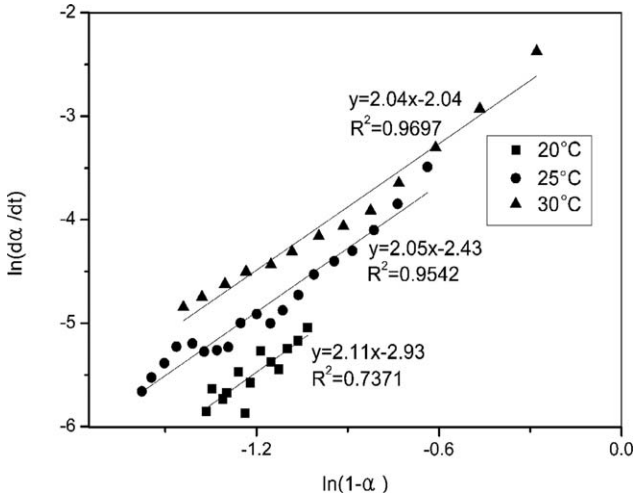


**Figure 9.** $\ln(1-\alpha)$ versus $\ln(d\alpha/dt)$ curves at different temperatures.

**Table III.** Values of $n$ and $k$ at Different Temperatures

| Temperature (°C) | $n$ | $k$ ($min^{-1}$) |
|---|---|---|
| 20 | 2.11 | 0.055 |
| 25 | 2.05 | 0.088 |
| 30 | 2.03 | 0.13 |

$$k=A\exp\left(\frac{-E_a}{RT}\right). \quad (5)$$

Taking the natural logarithm processing of both sides of the equation, we obtain

$$\ln k=\ln A-\left(\frac{E_a}{RT}\right). \quad (6)$$

Figure 10 shows the $\ln k$ versus $1/T$ curve.

Through linear fitting, $E_a = 63.52$ kJ/mol and $\ln A = 23.19$ were obtained.

On the basis of previous analysis results, the RTV-2-SEMR curing kinetics equation can be expressed as:

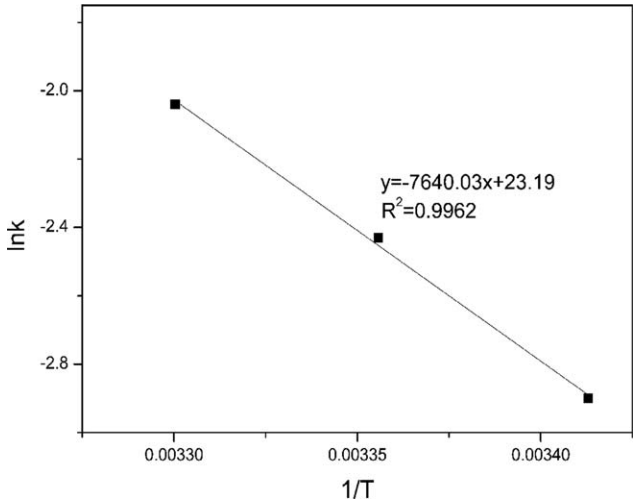


**Figure 10.** $\ln k$ versus $1/T$ curve.

**Table IV.** Calculated Curing Time and Measured Tack-Free Time at Different Temperatures

| Temperature (°C) | 20 | 25 | 30 |
|---|---|---|---|
| Measured tack-free time (min) | 90 | 60 | 40 |
| Calculated curing time (min) | 101 | 65 | 43 |

$$\frac{d\alpha}{dt} = k(1-\alpha)^2. \quad (7)$$

Integrating both sides of the equation, we obtain

$1/(1-\alpha) = kt + C$. When $t = 0$, $\alpha = 0$; thus, $C$ was computed as 1. The equation can finally be expressed as:

$$\frac{1}{(1-\alpha)} = kt + 1. \quad (8)$$

Combining this equation with Arrhenius equation, we obtain $\ln k = \ln A - (E_a/RT)$.

The new equation containing time ($t$), temperature ($T$), and conversion ($\alpha$) can be expressed as:

$$\ln t = \frac{7640}{T} - \ln\frac{1-\alpha}{\alpha} - 23.19. \quad (9)$$

Tack-free time is a very important time node. This time node should correspond to certain conversion. When $\alpha = 0.8$, 0.85, and 0.9, the corresponding curing time can be calculated at different temperatures. The calculation results showed that when $\alpha = 0.85$, the calculated curing time gave the closest agreement with the measured results.

Table IV shows the calculated curing time ($\alpha = 0.85$) and the measured tack-free time at different temperatures.

The results indicated that the calculated curing time ($\alpha = 0.85$) can be considered as the actual tack-free time with the optimized formula. The study of curing kinetics may serve as a theoretical basis for actual industrial applications.

## CONCLUSIONS

In this study, random copolymer PMES with different viscosities was synthesized through anionic ring-opening polymerization. Dehydrogenatively cross-linked RTV-2 silicone rubbers have been prepared using the PMES. The DMA results show that RTV-2 silicone rubbers have excellent low-temperature resistance, because there is no crystallization and they have a $T_g$ as low as −125°C. The mechanical properties of RTV-2 silicone rubbers with different formulas are investigated and the optimized formula was obtained. In addition, the curing kinetic analysis of RTV-2 silicone rubbers with optimized formula was conducted by monitoring *in situ* FTIR spectra over time. The results show that curing process is a second-order reaction, and the activation energy, pre-exponential factor, and reaction rate constant were obtained at different temperatures, then the kinetic eq. (9) could be derived. Calculation results indicate that when $\alpha = 0.85$, the calculated curing time gave the closest agreement with the experimentally measured tack-free time. The kinetic equation can be used to predict the tack-free time of this curing process at different temperatures.

## ACKNOWLEDGMENTS

This work was financially supported by the Special Fund for Shandong Independent Innovation and Achievements transformation (No. 2014ZZCX01101).

## REFERENCES

1. Kenji, T.; Shouei, F. *Polym. Bull.* **1999**, *43*, 129.
2. Martin, M.; Stefan, S.; Gerhard, K.; Dieter, O. *Makromol. Chem. Macromol. Symp.* **1990**, *34*, 171.
3. Yu, K. G.; Papkov, V. S. *Adv. Polym. Sci.* **1989**, *88*, 129.
4. Hsien, T. C.; Shih, H. C.; Jyh, H. W. *J. Appl. Polym. Sci.* **2003**, *89*, 959.
5. Out, G. J. J.; Turetskii, A. A.; Moeller, M.; Oelfin, D. *Macromolecules* **1994**, *27*, 3310.
6. Liu, L. H.; Yang, S. Y.; Zhang, Z. J.; Wang, Q.; Xie, Z. M. *J. Polym. Sci. Part A: Polym. Chem.* **2003**, *41*, 2722.
7. Brewer, J. R.; Tsuchihara, K.; Morita, R.; Jones, J. R.; Bloxsidge, J. P.; Kagao, S.; Otsuki, T.; Fujishige, S. *Polymer* **1994**, *35*, 5109.
8. Brewer, J. R.; Tsuchihara, K.; Morita, R.; Jones, J. R.; Bloxsidge, J. P.; Fujishige, S. *Polymer* **1994**, *35*, 5118.
9. Wiedemann, H. G.; Bernhard, W.; Joph, P. W. *Mol. Cryst. Liq. Cryst.* **1988**, *155*, 469.
10. Gerhard, K.; Alfred, H.; Martin, M. *Macromolecules* **1989**, *22*, 4190.
11. Cornelius, D. J.; Monroe, C. M. *Polym. Eng. Sci.* **1985**, *25*, 467.
12. Hideki, K.; Wataru, N. *Makromol. Chem.* **1993**, *194*, 1403.
13. Babu, G. N.; Christopher, S. S.; Newmark, R. A. *Macromolecules* **1987**, *20*, 2654.
14. Scheele, W. *Rubber Chem. Technol.* **1961**, *34*, 1306.
15. Scheele, W.; Cherubim, M. *Rubber Chem. Technol.* **1961**, *34*, 606.
16. Coran, A. Y. *Rubber Chem. Technol.* **1964**, *37*, 679.
17. James, R. W. *J. Appl. Polym. Sci.* **1968**, *12*, 1167.
18. James, R. W. *J. Appl. Polym. Sci.* **1968**, *12*, 1183.
19. Shyu, G. D.; Chan, T. W.; Isayev, A. I. *Rubber Chem. Technol.* **1994**, *67*, 314.
20. Prime, R. B. *Polym. Eng. Sci.* **1973**, *13*, 365.
21. Kamal, M. R.; Sourour, S. *Polym. Eng. Sci.* **1973**, *13*, 59.
22. Ishida, H.; Allen, D. J. *J. Polym. Sci. Part B: Polym. Phys.* **1996**, *34*, 1019.
23. Hu, D.; Zheng, S. *J. Appl. Polym. Sci.* **2011**, *119*, 2933.
24. Liu, P.; Song, J.; He, L.; Liang, X.; Ding, H. *J. Appl. Polym. Sci.* **2009**, *114*, 811.
25. Liu, L.; Yang, S.; Zhang, Z.; Wang, Q.; Xie, Z. *J. Polym. Sci. Part A: Polym. Chem.* **2003**, *41*, 2722.
26. Zhao, F.; Bi, W.; Zhao, S. *J. Macromol. Sci. Part B Phys.* **2011**, *50*, 1460.
27. Matthias, J.; Wolfgang, S.; Dietmar, W. *Polym. Test.* **2010**, *29*, 815.